Article

Sequence and Structure Dual-Dependent Interaction between Small Molecules and DNA for the Detection of Residual Silver Ions in As-Prepared Silver Nanomaterials

Zhaoyin Wang, Jian Zhao, Zijun Li, Jianchun Bao, and Zhihui Dai

Anal. Chem., **Just Accepted Manuscript** • Publication Date (Web): 23 May 2017

Sequence and Structure Dual-Dependent Interaction between Small Molecules and DNA for the Detection of Residual Silver Ions in As-Prepared Silver Nanomaterials

Zhaoyin Wang, Jian Zhao, Zijun Li, Jianchun Bao, and Zhihui Dai*

Jiangsu Collaborative Innovation Center of Biomedical Functional Materials and Jiangsu Key Laboratory of Biofunctional Materials, School of Chemistry and Materials Science, Nanjing Normal University, Nanjing, 210023, P. R. China

*Tel./Fax: +86-25-85891051. E-mail: daizhihuii@njnu.edu.cn.

ABSTRACT: Investigations on interaction between small molecules and DNA are the basis of designing advanced bioanalytical systems. We herein propose a novel interaction between heterocyclic aromatic compounds (HACs) and single-stranded DNA (ssDNA). Taking methylene blue (MB) as a typical HAC, it is found that MB can interact with cytosine (C)-rich ssDNA in an enthalpy-driven process. The interaction between MB and C-rich ssDNA is sequence and structure dual-dependent: at least three consecutive C and single-stranded structure are necessary. Except single-stranded structure, double-stranded, i-motif, and C-Ag-C mismatch structures will remarkably impede the interaction with MB. Uv-vis absorption, fluorescent, and electrochemical curves demonstrate that conjugated system, electron transition and electron transfer of MB are remarkably affected by MB-C-rich ssDNA interaction. In particular, the absorption peak of MB at 664 nm decreases, and a new peak at 538 nm emerges. Therefore, the interaction can be characterized by a colorimetric and ratiometric signal. Relying on inhibition of C-Ag-C mismatch and enhanced analytical performances of ratiometic signal, the MB-C-rich ssDNA interaction is further employed to quantify silver ions (Ag^+) selectively and sensitively. In addition, since silver nanomaterials cannot introduce C-Ag-C mismatch, the fabricated biosensor is able to sense residual Ag^+ in silver nanoparticles and silver nanowires, which is of great value in precise and economical preparation of silver nanomaterials.

INTRODUCTION

Nowadays, various silver nanomaterials (AgNMs) have been developed and applied in the realms of catalysis,[1] photochemistry,[2] optoelectronics,[3] medicine[4], and sensing[5,6]. Although AgNMs can be prepared with different methods,[7,8] a similar and fundamental procedure is reduction of silver ions (Ag^+). As a result, residual Ag^+ is inevitable in as-prepared AgNMs, which greatly affects subsequent applications and causes Ag^+ pollution. To address these issues, precise and economical preparation of AgNMs are urgently needed, which depends on methodologies that can detect Ag^+ in the presence of AgNMs. However, because of the interference from homologous nanostructures, distinction of residual Ag^+ in as-prepared AgNMs meet great challenges. To date, analytical protocols that could fulfill the stringent demands are still rare.[9,10]

As the foundational material of living organisms and nanotechnology, DNA is intrinsically linked to diverse processes both in vivo and in vitro.[11-13] Some small molecules can interact with DNA, and consequently regulate DNA-related biological procedures and DNA-based nano-architecture.[14,15] Among these small molecules, heterocyclic aromatic compounds (HACs) are considered to be the promising ones due to their broad applications.[16,17] For instance, HACs can accomplish cell imaging and photodynamic therapy by HACs-DNA interaction.[18,19] Besides, relying on their unique optical and electrical properties, HACs have been widely used to develop numerous DNA-based biosensors as probe molecules.[20-23]

Specific interactions between HACs and DNA are the basis of designing advanced bioanalytical systems. To our knowledge, HACs mainly interact with double-stranded DNA (dsDNA) in three different manners[24]: structure-dependent manner (groove interaction[25] and G-quadruplex interaction[26,27]), base pair-dependent manner (intercalative interaction)[28] and charge-dependent manner (electrostatic interaction)[29]. However, the explanations of these interactions are diverse and sometimes irreconcilable. For instance, it has been demonstrated that MB can bind to both alternating GC base sequence and alternating AT base sequence.[30,31] More importantly, bases in dsDNA are hybridized and cannot freely participate in the interaction with HACs. Therefore, the effect of base in these manners is notably covered. Single-stranded DNA (ssDNA) can be recognized as a polymer with bases along its negative-charged backbone.[32] Actually, ssDNA has some features that favor its interaction between bases and HACs. First, bases themselves are HACs, and thus have similar structures with other HACs. Second, ssDNA is much more flexible than dsDNA,[33] which is critical to survey possible synergistic effect of bases. Besides, bases in

ssDNA are free in orientation and can provide many groups to build various links with other molecules.[34] All these properties indicate great potential of discovering novel interaction manners between HACs and ssDNA.

In this work, for the first time, we report a specific interaction be-tween HACs and cytosine (C)-rich ssDNA. The interaction is highly related to the sequence of ssDNA, in which at least three consecutive Cs are required, and more consecutive Cs will intensify the interaction. Except for single-stranded structure, C-rich DNA can be employed to form other structures that will remarkably impede the interaction with HACs. That means this interaction manner is sequence and structure dual-dependent. Moreover, because of the effect of ssDNA on conjugated system, electron transition and electron transfer, colorimetric, fluorescent and electrochemical behaviors of HACs are significantly affected. To be noted, after the interaction with ssDNA, typical ab-sorption peaks of HACs decrease, and new ones emerge. Therefore, the interaction can be characterized by a colorimetric and ratiometric signal that is further employed to design an Ag^+ biosensor. In addition, different from Ag^+, silver nanomaterials cannot introduce C-Ag-C mismatch in C-rich ssDNA, thus the fabricated biosensor is able to sense residual Ag^+ in unpurified silver nanoparticles (AgNPs) and silver nanowires (AgNWs).

EXPERIMENTAL SECTION

Chemicals and Materials. Methylene blue (MB), acridine orange hemi(zinc chloride) salt, methylene green zinc chloride double salt, cresyl violet acetate, thionin acetate, silver nitrate ($AgNO_3$), sodium borohydride ($NaBH_4$), Tris(2-carboxyethyl)phosphine hydrochloride (TCEP), trisodium citrate, ethylenediaminetetraacetic acid disodium salt dehydrate (EDTA), tris(hydroxymethyl)aminomethane (Tris), and deoxynucleotide were purchased from Sigma-Aldrich. All other chemicals used in this work were of analytical grade and directly used without additional purification. All oligonucleotides (HPLC purified, sequences shown in Table S1) were obtained from TaKaRa Inc. (Dalian, China). All solutions were prepared with ultrapure water (18.2 MΩ•cm) from a Milli-Q purification system (Bedford, MA).

Colorimetric and fluorescent measurements. Except for special statement, DNA and HACs were dissolved in TE buffer (10 mM Tris, 1 mM EDTA, pH 8.0) with final concentrations of 10 μM and 100 μM, respectively. To observe the interaction between MB and C-rich ssDNA, 20 μL DNA and 50 μL MB were mixed with 130 μL Tris-HCl buffer. Then, the color of solution changed immediately and a purple solution was obtained in 10 minutes, which was ready for colorimetric and fluorescent characterization. To test the versatility of this interaction, acridine orange, methylene green, cresyl violet and thionin were used in preparing samples. To test the effect of pH, DNA and MB were dissolved in different TE buffer (pH 6.0 7.0 8.0 9.0, and 10.0). To test the effect of ionic strength, DNA and MB were dissolved in TE buffer (pH 8.0) that contained different concentrations of KCl.

Electrochemical measurement. Pretreatment of working electrode was carried out according to previously reported literature.[35] 40 μL of 5 μM thiolated DNA was firstly mixed with 10 μL of 10 mM TCEP to reduce the disulfide bond. After that, 6 μL DNA solution was dropped onto the freshly cleaned electrode surface. The electrode was kept at 4 ºC for 16 h to form a self-assembled monolayer of DNA. Then, the electrode was reacted with 1 mM MCH for 2 h in darkness to fill the pinholes in the monolayer. Afterward, the DNA modified electrode was immersed into an electrolyte that contained 10 μM MB for 10 minutes. Cyclic voltammetric measurement was carried out on a CHI660D potentiostat (China) in the potential range of -0.5 V-0.0 V with a scan rate of 50 $mV•s^{-1}$. Before the measurement, the electrolyte was firstly bubbled thoroughly with high purity nitrogen for 30 min. Then a stream of nitrogen was blown gently across the surface of the solution in order to maintain the solution anaerobic throughout the experiment.

Isothermal titration calorimetry (ITC). ITC measurement was carried out by a TAM 2277-201 microcalorimetric system (Thermometric AB, Järfalla, Sweden). The sample cell was initially loaded with 600 μL of 10 μM DNA. Subsequently, 330 μL of 1 M MB was injected dropwise (5 μL) into the stirred sample cell. All the measurements were performed at room temperature (25.00 ± 0.01°C).

Circular dichroism (CD). CD was employed to confirm the structures of DNA. To obtain double-stranded and metal-induced mismatch structures, poly(24G) and silver ions were mixed with ploy(24C), respectively. To obtain an i-motif structure, ploy(24C) was dissolved and prepared under the condition of pH 6.0. Afterward, the as-prepared solutions were heated up to 90 °C for 5 min and then slowly cooled down to room temperature. CD measurements were carried out on a digital Circular Dichroism Spectrometer (Britain, Applied Photophysics) using quartz cells and a 1 nm band width, 1 nm step size, 10 mm path length. The scan range was from 350 nm to 200 nm. All the experiments were performed at room temperature.

RESULTS AND DISCUSSION

Interaction between methylene blue (MB) and C-rich ssDNA. MB is a model HAC that is widely utilized in studying the interaction between small molecules and DNA. In this work, we also choose MB as the representative molecule to explore novel HAC-DNA interaction (Figure 1A). In solution, MB exists in two forms: monomer MB and dimer MB, which have characteristic absorption peaks at 664 nm and 605 nm (Figure 1B),[36] respectively. Despite the fact that the monomer-dimer equilibrium of MB at different concentrations constantly reconstructs, the color of MB solution keeps in blue (Figure S1). However, when C-rich ssDNA is added into MB solution, the color immediately changes from blue to light purple (inset photograph in Figure 1B). Accompanied with the color change, the peaks at 664 nm and 605 nm decrease, while a new peak at 538 nm emerges. This means the monomer and dimer MB in solution are consumed, and an interaction between MB and C-rich ssDNA occurs. Compared with the original peaks (664 nm and 605 nm), emerged peak (538 nm) is blue-shift, suggesting the conjugated system of MB is enlarged after interacting with C-rich ssDNA. The interaction between MB and C-rich ssDNA has also been confirmed by isothermal titration calorimetry (ITC) (Figure 1C and Figure 1D). In comparison with fitting curves of poly(24A) and poly(24T) (Figure S2A and Figure S2B), the fitting curve of poly(24C) is significantly different. Although the fitting curves of poly(24C) and poly(24G) are similar, ΔH and ΔS of MB-poly(24C) interaction are -31.81 KJ/mol and -20.91 J/mol, while those of MB-poly(24G) interaction are -

18.86 KJ/mol and 32.33 J/mol. That is to say, the interaction between MB and poly(24C) is enthalpy-driven and entropically unfavorable, and the interaction between MB and poly(24G) is driven by both enthalpy and entropy. Accordingly, it can be concluded that MB interacts with poly(24C) in a new manner. By replacing MB with four other HACs (i.e., methylene green, thionin, cresyl violet and acridine orange), distinct differences in Uv-vis absorption spectra are also observed (Figure S3), indicating the versatility of this interaction.

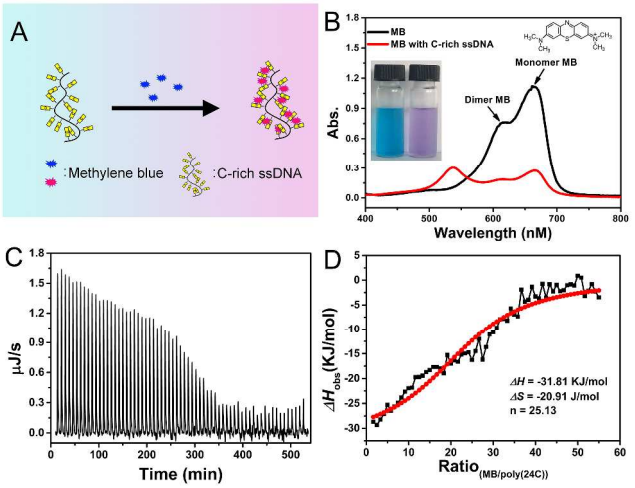

Figure 1. (A) Schematic representation of the interaction between MB and C-rich ssDNA. (B) Uv-vis absorption spectra of MB and MB with C-rich ssDNA. Insets: the corresponding photograph of MB and MB with C-rich ssDNA, and two-dimensional structure of MB. (C) ITC curve by titrating poly(24C) with MB. (D) Observed enthalpy Δ_{Hobs} of MB/poly(24C) solution plotted against the molar fraction of MB/poly(24C).

Sequence and structure dual-dependent property of the interaction. Sequence-dependent property of the interaction between MB and C-rich ssDNA is first identified. As mentioned above, DNA can interact with HAC in several manners. In Figure 2A, a new peak at 538 nm can be found after the interaction between poly(24C) and MB, indicating that the manner of poly(24C)-MB interaction is different from that of poly(24A)-MB interaction, poly(24G)-MB interaction and poly(24T)-MB interaction. By replacing poly(24C) with its corresponding base (C), the interaction cannot be observed (Figure 2B). These results demonstrate that the interaction between MB and poly(24C) depends on the synergistic effect of consecutive C rather than single C. Besides, it is found that the number of consecutive C also greatly affects the interaction. If the number of consecutive C is less than 2 (poly(CT) and poly(CCT)), MB cannot interact with these ssDNA (Figure 2C). When the number of consecutive C is up to 3 (poly(CCCT)), the peak at 538 nm begins to emerge. As the number of consecutive C further increases, the interaction is dramatically improved. In comparison with poly(24C) and poly(12C), it can be found that the capability of interacting with MB is correlative with the amount of C in ssDNA (Figure S4A and Figure S4B). For poly(24C) and MB, the optimized concentrations of MB and DNA are 25 μM and 1μM (Figure S5A and Figure S5B), respectively. That means one poly(24C) can react with 25 MB, which is fit well with the results of ITC (n = 25.13). Since there are 24 consecutive C in poly(24C), it can be calculated that the ratio of C and MB is about 1.

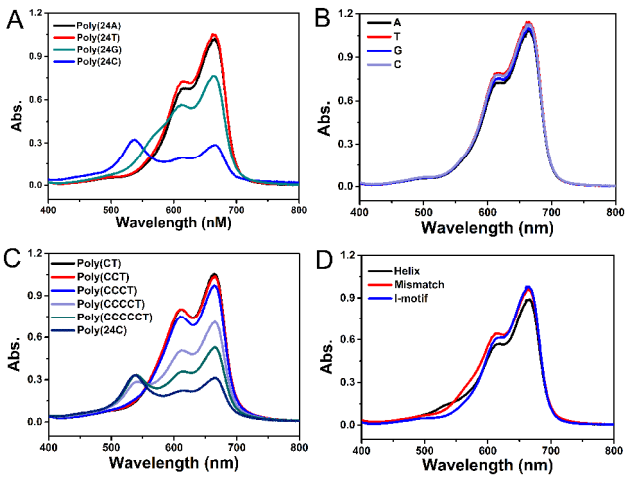

Figure 2. (A) Uv-vis absorption spectra of MB with poly(24A), poly(24T), poly(24G) and poly(24C). (B) Uv-vis absorption spectra of MB with A, T, G and C. (C) Uv-vis absorption spectra of MB with poly(CT), poly(CCT), poly(CCCT), poly(CCCCT), poly(CCCCCT) and poly(24C). (D) Uv-vis absorption spectra of MB with double-stranded, mismatch and i-motif structures formed by poly(24C).

Structure-dependent property of this interaction is further confirmed. SsDNA can form double-stranded structure by hybridizing with its complementary strand. For C-rich ssDNA, it can form i-motif structure at acidic pH. Besides, mismatch structure of C-rich ssDNA occurs with the help Ag^+. We identify the double-stranded, mismatch and i-motif structures with circular dichroism (Figure S6). When these three structures are mixed with MB, no evident interaction is observed (Figure 2D). At neutral and alkaline pH, C-rich DNA keeps in single-stranded structure, and can interact with MB. Notably, the intensity of interaction at alkaline pH is stronger than that at neutral pH (Figure S7A). Since ionic strength can affect the stability of DNA structure, effect of ionic strength on the interaction has also been investigated. As shown in Figure S7B, there are significant interactions between MB and C-rich ssDNA under a broad range of KCl concentration (0 to 100 mM). As proved above, the interaction between MB and C-rich ssDNA relies on the synergistic effect of bases. In ssDNA, bases are exposed outside, facilitating the interaction with MB, while bases are occupied by forming other structures. Therefore, MB can only interact with ssDNA, verifying the structure-dependent property of this interaction manner. In combination with its sequence-dependent property, the novel interaction manner possesses desirable dual-dependent property.

Effect of the interaction on fluorescent and electrochemical behaviors of MB. As shown in Figure 3A, MB has a typical fluorescence intensity curve with the maximum emission at 691 nm and the maximum excitation at 664 nm. However, after interacting with C-rich ssDNA, the fluorescence of MB is significantly quenched. Meanwhile, the maximum emission is slightly blue-shift (from 691 nm to 685 nm), reflecting the impediment of the electronic transition of MB by C-rich ssDNA. By mixing DNA with different concentrations of MB, it can be found that blue-shift of maximum

emission occurs at the low concentrations of MB (Figure S8). Electrochemical behaviors of MB are also affected by C-rich ssDNA. MB can absorb onto the negative-charged backbone of ssDNA, and the electron can transfer along the ssDNA, resulting in defined redox peaks of MB (Poly(24T) curve in Figure 3B). However, on poly(24C)-modified electrode surface, both reductive and oxidative peaks of MB remarkably increase, reflecting that more MB is assembled by C-rich ssDNA. Moreover, two noteworthy differences of poly(24C) curve and poly(24T) curve should be pointed out. First, the increments of cathodic peak current (Δipc) and anodic peak current (Δipa) are not equal. Second, in comparison with poly(24T) curve, ΔEp (difference of cathodic and anodic peak potential) of poly(24C) curve is enlarged, suggesting the electron transfer is depressed. These results prove that the route of electron transfer between MB and poly(24C)-modified electrode is different from that between MB and poly(24T)-modified electrode.

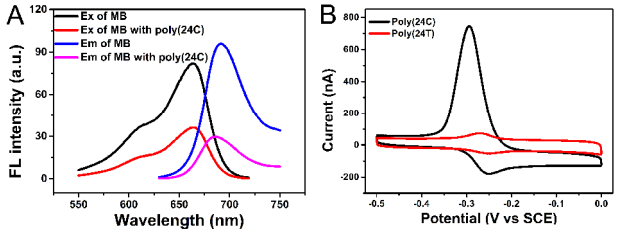

Figure 3. (A) Excitation and emission curves of MB and MB with poly(24C). (B) Cyclic voltammetric curves of MB on poly(24T)-modified electrode and poly(24C)-modified electrode.

Fabrication of Ag^+ biosensor based on the interaction between MB and C-rich ssDNA. We finally design a facile Ag^+ colorimetric biosensor to confirm the applicability of this HAC-DNA interaction for the following reasons. First, the interaction between HACs and C-rich ssDNA can be accomplished in a few minutes, resulting in a significant color change. Therefore, the detection results can be obtained by naked eyes in a short time, which is of great value in point-of-care and field use testing. Besides, accompanied with the HAC-DNA interaction, there are disappearance of the original peaks and appearance of a new peak, providing ratiometric signals to quantify the intensity of this interaction.

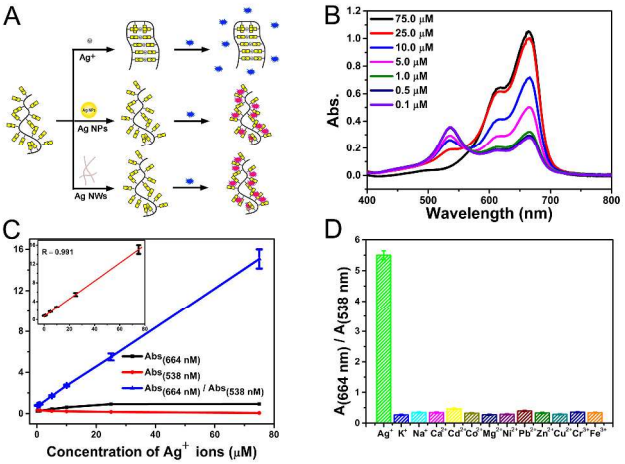

Figure 4. (A) Schematic representation of a colorimetric Ag^+ biosensor and its application in two kinds of silver nanomaterials (Ag NMs). (B) UV-vis absorption spectra of MB and poly(24C) with different concentration of Ag^+. (C) Calibration curve for absorption values ($A_{664\ nm}$ and $A_{538\ nm}$) and ratiometric absorption value ($A_{664\ nm}/A_{538\ nm}$) versus Ag^+ concentrations. Inset: a linear range of Ag^+ concentration from 0.1 to 75 μM. (D) The selective performance of this biosensor. The concentration of tested metal ions is 50 μm.

The principle of this biosensor has been illustrated in Figure 4A. Ag^+ can introduce C-Ag-C mismatch in C-rich ssDNA, which will inhibit the interaction between DNA and MB, keeping the color of detection system blue. On the contrary, in the absence of Ag^+, C-rich ssDNA will interact with MB, changing the color into purple. Therefore, quantification of Ag^+ is achieved by monitoring the change of color, which can be correctly recorded by Uv-vis absorption spectra (Figure 4B). Specifically, as the concentration of Ag^+ increases, the absorption peaks at 664 nm and 538 nm decrease and increase, respectively. Figure 4C indicates the advantage of ratiometric signal in promoting the analytical performances of this biosensor. Taking $A_{664\ nm}$ as a characteristic signal, Ag^+ can be detected in a linear range from 0.5 to 25 μM with the detection limit of 350 nM. Similarly, taking $A_{538\ nm}$ as a characteristic signal, a linear range from 1 to 25 μM and a detection limit of 590 nM are obtained. If taking $A_{664\ nm}/A_{538\ nm}$ as a characteristic signal, the value of ratiometric signals is proportional to the Ag^+ concentration in the range from 0.1 to 75 μM (the inset of Figure 4C). The regression equation is $A_{664\ nm}/A_{538\ nm}$ = 0.70 + 0.19C(Ag^+) (μM), R = 0.991. The detection limit of this Ag^+ biosensor is calculated to be 58 nM (S/N = 3). The selectivity of this biosensor was verified by challenging the biosensor with other metal ions. As shown in Figure 4D, a significant difference of the ratiometric signal can be observed for the Ag^+ and other metal ions, indicating satisfactory selectivity of the colorimetric Ag^+ biosensor.

Quantification of residual Ag^+ in as-prepared AgNMs. The proposed biosensor is further challenged in sensing residual Ag^+ in as-prepared AgNMs. We synthesize two kinds of AgNMs (*i.e.*, AgNPs and AgNWs) according to previously reports,[37,38] and test the feasibility of our biosensor in these samples. If Ag NMs are purified to eliminate Ag^+ in advance, interaction between MB and C-rich ssDNA is observed (Figure S9). However, unpurified Ag NMs will block the interaction, due to the residue of Ag^+. Table 1 exhibits the results of quantification of Ag^+ in Ag NMs based on the interaction between MB and C-rich ssDNA. High recovery percentage and low relative standard deviation (RSD) indicate that Ag^+ can be accurately determined in the presence of AgNMs.

Table 1. Determination of residual Ag^+ ions in as-prepared AgNPs and AgNWs using the proposed biosensor.

	Ag^+ added (μM)	Ag^+ found (μM)	Recovery (%)	RSD (%, n = 3)
AgNPs	0.0	2.4	N/A[a]	5.3
	0.5	3.0	120.0	4.6
	5.0	7.6	104.0	3.8
	50.0	53.5	102.2	3.1

AgNWs	0.0	7.6	N/A	2.3
	0.5	8.2	120.0	4.5
	5.0	13.1	110.0	3.9
	50.0	60.2	105.2	3.2

[a] N/A represents Not Applicable.

CONCLUSION

In summary, a novel sequence and structure dual-dependent HAC-DNA interaction is reported in this work. Specifically, to achieve the interaction, DNA should contain C-rich sequence and the structure of DNA should be single-stranded. Systematic investigation demonstrates that it is the synergistic effect of consecutive C in ssDNA that results in the interaction. Meanwhile, after interacting with C-rich ssDNA, the conjugated systems of HACs are enlarged, and the electron transition and transfer of HACs are depressed. As a result, colorimetric, fluorescent and electrochemical behaviors of HACs are significantly affected. Based on these principles, a facile colorimetric Ag^+ biosensor is fabricated as an example to confirm the applicability of this HAC-DNA interaction. Relying on the desirable retiometric signals, the proposed biosensor reveals the feasibility of quantifying residual Ag^+ in AgNPs and AgNWs, which will deepen the understanding of AgNMs preparation, and thus facilitate the applications of AgNMs and reduce Ag^+ pollution.

ASSOCIATED CONTENT

Supporting Information

The Supporting Information is available free of charge on the ACS Publications website.

Detailed sequences of oligonucleotides used in this work (Table S1); Uv-vis absorption spectra of MB, HACs with C-rich ssDNA, and MB with pretreated C-rich ssDNA (Figure S1, S3, and S9); ITC curves of MB with different DNA (Figure S2); Effect of C-rich length, concentration, pH, and ionic strength on MB-C-rich ssDNA interaction (Figure S4, S5, and S7); CD spectra of C-rich ssDNA under different conditions (Figure S6); Emission curves of C-rich ssDNA with different concentrations of MB (Figure S8).

AUTHOR INFORMATION

Corresponding Author

*Tel./Fax: +86-25-85891051. E-mail: daizhihuii@njnu.edu.cn.

ORCID

Zhihui Dai: 0000-0001-7049-7217

Notes

The authors declare no competing financial interest.

ACKNOWLEDGMENT

This work was supported by the National Natural Science Foundation of China for Projects 21625502, 21475062, 21533012 and 21505077 and PAPD.

REFERENCES

(1) Zugic, B.; Wang, L.; Heine, C.; Zakharov, D. N.; Lechner, B. A. J.; Stach, E. A.; Biener, J.; Salmeron, M.; Madix, R. J.; Friend, C. M. *Nat. Mater.* **2016**, DOI: 10.1038/NMAT4824.
(2) Cao, Y. T.; Geng, W.; Shi, R.; Shang, L.; Waterhouse, G. I. N.; Liu, L. M.; Wu, L. Z.; Tung, C. H.; Yin, Y. D.; Zhang, T. R. *Angew. Chem. Int. Edit.* **2016**, *55*, 14952-14957.
(3) Lee, H.; Kim, M.; Kim, I.; Lee, H. *Adv. Mater.* **2016**, *28*, 4541-4548.
(4) Yang, X. X.; Li, C. M.; Huang, C. Z. *Nanoscale* **2016**, *8*, 3040-3048.
(5) Ma, J. L.; Yin, B. C.; Wu, X.; Ye, B. C. *Anal. Chem.* **2017**, *89*, 1323-1328.
(6) Wang, P.; Bai, Y.; Yao, C.; Li, X.; Zhou, L.; Wang, W.; El-Toni, A. M.; Zi, J.; Zhao, D.; Shi, L.; Zhang, F. *Anal. Chem.* **2017**, *89*, 2583-2591.
(7) Panacek, A.; Prucek, R.; Hrbac, J.; Nevecna, T.; Steffkova, J.; Zboril, R.; Kvitek, L. *Chem. Mater.* **2014**, *26*, 1332-1339.
(8) Bai, W. S.; Sheng, Q. L.; Ma, X. Y.; Zheng, J. B. *Acs Sustain. Chem. Eng.* **2015**, *3*, 1600-1609.
(9) Gonzalez-Fuenzalida, R. A.; Moliner-Martinez, Y.; Gonzalez-Bejar, M.; Molins-Legua, C.; Verdu-Andres, J.; Perez-Prieto, J.; Campins-Falco, P. *Anal. Chem.* **2013**, *85*, 10013-10016.
(10) Huang, K.; Xu, K. L.; Tang, J.; Yang, L.; Zhou, J. R.; Hou, X. D.; Zheng, C. B. *Anal. Chem.* **2015**, *87*, 6584-6591.
(11) Krishnan, S.; Simmel, F. C. *Nat. Chem.* **2015**, *7*, 17-18.
(12) Li, J.; Hong, C. Y.; Wu, S. X.; Liang, H.; Wang, L. P.; Huang, G. M.; Chen, X.; Yang, H. H.; Shangguan, D. H.; Tan, W. H. *J. Am. Chem. Soc.* **2015**, *137*, 11210-11213.
(13) Wu, C. C.; Cansiz, S.; Zhang, L. Q.; Teng, I. T.; Qiu, L. P.; Li, J.; Liu, Y.; Zhou, C. S.; Hu, R.; Zhang, T.; Cui, C.; Cui, L.; Tan, W. H. *J. Am. Chem. Soc.* **2015**, *137*, 4900-4903.
(14) Avakyan, N.; Greschner, A. A.; Aldaye, F.; Serpell, C. J.; Toader, V.; Petitjean, A.; Sleiman, H. F. *Nat. Chem.* **2016**, *8*, 368-376.
(15) Li, J.; Fan, C. H.; Pei, H.; Shi, J. Y.; Huang, Q. *Adv. Mater.* **2013**, *25*, 4386-4396.
(16) Anders, L.; Guenther, M. G.; Qi, J.; Fan, Z. P.; Marineau, J. J.; Rahl, P. B.; Loven, J.; Sigova, A. A.; Smith, W. B.; Lee, T. I.; Bradner, J. E.; Young, R. A. *Nat. Biotechnol.* **2014**, *32*, 92-96.
(17) Doan, P. H.; Pitter, D. R. G.; Kocher, A.; Wilson, J. N.; Goodson, T. *J. Am. Chem. Soc.* **2015**, *137*, 9198-9201.
(18) Ethirajan, M.; Chen, Y. H.; Joshi, P.; Pandey, R. K. *Chem. Soc. Rev.* **2011**, *40*, 340-362.
(19) Sgambellone, M. A.; David, A.; Garner, R. N.; Dunbar, K. R.; Turro, C. *J. Am. Chem. Soc.* **2013**, *135*, 11274-11282.
(20) Lou, C.; Dallmann, A.; Marafini, P.; Gao, R.; Brown, T. *Chem. Sci.* **2014**, *5*, 3836-3844.
(21) Yang, A. H. J.; Hsieh, K.; Patterson, A. S.; Ferguson, B. S.; Eisenstein, M.; Plaxco, K. W.; Soh, H. T. *Angew. Chem. Int. Edit.* **2014**, *53*, 3163-3167.
(22) Kekedy-Nagy, L.; Shipovskov, S.; Ferapontova, E. E. *Anal. Chem.* **2016**, *88*, 7984-7990.
(23) Du, Y.; Dong, S. J. *Anal. Chem.* **2017**, *89*, 189-215.
(24) Pichon, A.; Turro, C. *Nat. Chem.* **2012**, *4*, 591-591.
(25) Wei, D. G.; Wilson, W. D.; Neidle, S. *J. Am. Chem. Soc.* **2013**, *135*, 1369-1377.
(26) Collie, G. W.; Promontorio, R.; Hampel, S. M.; Micco, M.; Neidle, S.; Parkinson, G. N. *J. Am. Chem. Soc.* **2012**, *134*, 2723-2731.
(27) Chung, W. J.; Heddi, B.; Hamon, F.; Teulade-Fichou, M. P.; Phan, A. T. *Angew. Chem. Int. Edit.* **2014**, *53*, 999-1002.
(28) Fung, S. K.; Zou, T. T.; Cao, B.; Chen, T. F.; To, W. P.; Yang, C.; Lok, C. N.; Che, C. M. *Nat. Commun.* **2016**, *7*, 10655.
(29) Masetti, M.; Xie, H. N.; Krpetic, Z.; Recanatini, M.; Alvarez-Puebla, R. A.; Guerrini, L. *J. Am. Chem. Soc.* **2015**, *137*, 469-476.
(30) Rohs, R.; Sklenar, H.; Lavery, R.; Ro1der. B. *J. Am. Chem. Soc.* **2000**, *122*, 2860-2866.
(31) Rohs, R.; Sklenar, H. *J. Biomol. Struct. Dyn.* **2004**, 21, 699-711.
(32) Mason, J. A.; Laramy, C. R.; Lai, C. T.; O'Brien, M. N.; Lin, Q.

Y.; Dravid, V. P.; Schatz, G. C.; Mirkin, C. A. *J. Am. Chem. Soc.* **2016**, *138*, 8722-8725.
(33) Yang, D. Y.; Hartman, M. R.; Derrien, T. L.; Hamada, S.; An, D.; Yancey, K. G.; Cheng, R.; Ma, M. L.; Luo, D. *Accounts Chem. Res.* **2014**, *47*, 1902-1911.
(34) Jones, M. R.; Seeman, N. C.; Mirkin, C. A. *Science* **2015**, *347*, 1260901.
(35) Zhang, J.; Song, S. P.; Wang, L. H.; Pan, D.; Fan, C. H. *Nat. Protoc.* **2007**, *2*, 2888-2895.
(36) Zhang, S. L.; Chu, Z. Q.; Yin, C.; Zhang, C. Y.; Lin, G.; Li, Q. *J. Am. Chem. Soc.* **2013**, *135*, 5709-5716.
(37) Wei, T. X.; Dong, T. T.; Wang, Z. Y.; Bao, J. C.; Tu, W. W.; Dai, Z. H. *J. Am. Chem. Soc.* **2015**, *137*, 8880-8883.
(38) Garnett, E. C.; Cai, W. S.; Cha, J. J.; Mahmood, F.; Connor, S. T.; Christoforo, M. G.; Cui, Y.; McGehee, M. D.; Brongersma, M. L. *Nat. Mater.* **2012**, *11*, 241-249.

for TOC only